

Algorithms for Producing Linear Dilution Gradient with Digital Microfluidics

Sukanta Bhattacharjee*, Ansuman Banerjee*, Tsung-Yi Ho[†], Krishnendu Chakrabarty[‡], and Bhargab B. Bhattacharya*

*Nanotechnology Research Triangle, Indian Statistical Institute, Kolkata 700108, India, E-mail: {sukanta_r, ansuman, bhargab}@isical.ac.in

[†]Dept. CS & Inform. Engg., National Cheng Kung University, Tainan, Taiwan 70101, E-mail: tyho@csie.ncku.edu.tw

[‡]Dept. ECE, Duke University, Durham, NC 27708, USA, E-mail: krish@ee.duke.edu

Abstract—Digital microfluidic (DMF) biochips are now being extensively used to automate several biochemical laboratory protocols such as clinical analysis, point-of-care diagnostics, and polymerase chain reaction (PCR). In many biological assays, e.g., in bacterial susceptibility tests, samples and reagents are required in multiple concentration (or dilution) factors, satisfying certain “gradient” patterns such as linear, exponential, or parabolic. Dilution gradients are usually prepared with continuous-flow microfluidic devices; however, they suffer from inflexibility, non-programmability, and from large requirement of costly stock solutions. DMF biochips, on the other hand, are shown to produce, more efficiently, a set of random dilution factors. However, all existing algorithms fail to optimize the cost or performance when a certain gradient pattern is required. In this work, we present an algorithm to generate any arbitrary linear gradient, on-chip, with minimum wastage, while satisfying a required accuracy in the concentration factor. We present new theoretical results on the number of *mix-split* operations and *waste* computation, and prove an upper bound on the storage requirement. The corresponding layout design of the biochip is also proposed. Simulation results on different linear gradients show a significant improvement in sample cost over three earlier algorithms used for the generation of multiple concentrations.

I. INTRODUCTION

Recent advances in digital microfluidic (DMF) biochips have enabled realizations of a variety of laboratory assays on a tiny chip for automatic and reliable analysis of biochemical samples. A DMF biochip consists of a patterned 2D array or a customized layout of electrodes, typically a few square centimeters in size [1], [2]. The device can manipulate pico- or femtoliter-sized discrete droplets for the purpose of conducting various fluidic operations under electrical actuations. Typical fluidic operations on a droplet include dispensing, transport, mixing, splitting, heating, incubation, and sensing [3], [4], [5], [6]. DMF biochips offer significant flexibility and programmability over their continuous-flow counterparts while implementing various assays that mandate high-sensitivity, and low requirement of sample and reagent consumption. One such example is sample preparation, which plays a pivotal role in biochemical laboratory protocols, e.g., in polymerase chain reaction (PCR) [7], and in other applications in biomedical engineering and life sciences [8], [9], [10], [11], [12]. An important step in sample preparation is dilution, where the objective is to prepare a fluid with a desired concentration (or dilution) factor. There are two performance metrics in sample preparation: the number of *mix-split* operations to achieve a concentration factor with a specified accuracy, and

the overall reactant usage (equivalently, waste production). The first parameter determines the sample preparation time, whereas the latter is related to the cost of stock solution. An efficient sample preparation algorithm should target to minimize either one or both of them as far as possible.

In sample preparation, producing chemical and biomolecular concentration gradients is of particular interest. Dilution gradients play essential roles in in-vitro analysis of many biochemical phenomena including growth of pathogens and selection of drug concentration. For example, in drug design, it is important to determine the minimum amount of an antibiotic that inhibits the visible growth of bacteria isolate (defined as minimum inhibitory concentration (MIC)). The drug with the least concentration factor (i.e., with highest dilution) that is capable of arresting the growth of bacteria, is considered as MIC. During the past decade, a variety of automated bacterial identification and antimicrobial susceptibility test systems have been developed, which provide results in only few hours rather than days, compared to traditional overnight procedures [9]. Typical automated susceptibility methods use an exponential dilution gradient (e.g., 1%, 2%, 4%, 8%, 16%) in which concentration factors (\mathcal{CF}) of the given sample are in geometric progression [8]. Linear dilution gradient (e.g., 15%, 20%, 25%, 30%, 35%), in which the concentration factors of the sample appear in arithmetic progression, offers more sensitive tests. Linear gradients are usually prepared by using continuous-flow microfluidic ladder networks [13], or by other networks of microchannels [14], [15]. Since the fluidic microchannels are hardwired, continuous-flow based diluters are designed to cater to only a pre-defined gradient, and thus they suffer from inflexibility and non-programmability. Also, these methods require a significant amount of costly stock solutions. In contrast, on a DMF biochip platform, a set of random dilution factors can be easily prepared. However, existing algorithms [16], [17], [18] fail to optimize the cost or performance when a certain gradient pattern is required.

In digital microfluidics, two types of dilution methods are used: serial dilution and interpolated dilution [19]. A serial dilution consists of a sequence of simple dilution steps to reduce the concentration of a sample. The source of the dilution sample for each step comes from the diluted sample of the previous step. A typical serial procedure generates an *exponential dilution* profile, in which, a unit volume sample/reagent droplet is mixed with a unit-volume buffer (0%) droplet to obtain

dilution gradient with minimum wastage (reagent consumption is minimum). To illustrate the proposed algorithm we assume that the two boundary concentrations (first and last \mathcal{CF} s of the target sequence) are available. If droplets with the two boundary \mathcal{CF} s are not supplied, we can prepare them by diluting the original (100%) sample with a buffer (0%) following an earlier algorithm [23], [24]. A simple observation that motivates us to design the proposed linear gradient generator is the following: mixing two non-consecutive \mathcal{CF} s, which are separated by an odd number of elements of the gradient sequence, produces the median of the two concentrations. This special property follows from the simple fact that the \mathcal{CF} values in the linear gradient sequence are in arithmetic progression. This property is used to design our algorithm for producing the gradient with no wastage. Moreover, only the concentrations that are elements of the gradient set will be generated during this process.

IV. PROBLEM FORMULATION

The problem of linear dilution sample preparation can be formulated as follows. Let $\mathcal{L} = \{\frac{a}{2^n}, \frac{a+d}{2^n}, \frac{a+2d}{2^n}, \dots, \frac{a+2^k d}{2^n}\}$ be a linear gradient of targets to be generated from $\frac{0}{2^n}$ and $\frac{2^n}{2^n}$, i.e., $|\mathcal{L}| = 2^k + 1$. Our objective is to generate all \mathcal{CF} values of \mathcal{L} without generating any waste droplets; we assume that a sufficient supply of boundary concentrations ($\frac{a}{2^n}$ and $\frac{a+2^k d}{2^n}$) is available.

A. Zero-waste linear dilution gradient

The process of generating the target \mathcal{CF} s satisfying a linear dilution gradient can be envisaged as a tree structure called linear dilution tree (LDT), as described below.

Algorithm 1: Build linear dilution tree (LDT)

Input: A set of \mathcal{CF} s (\mathcal{L})
Output: Root of the linear dilution tree

- 1 **if** \mathcal{L} contains only one \mathcal{CF} **then**
- 2 Create a leaf v storing this point;
- 3 **else**
- 4 Let C_{mid} be the median of \mathcal{L} ;
- 5 Set $L_{left} = \mathcal{CF}$ s less than C_{mid} in \mathcal{L} ;
- 6 Set $L_{right} = \mathcal{CF}$ s greater than C_{mid} in \mathcal{L} ;
- 7 $v_{left} = LDT(L_{left})$;
- 8 $v_{right} = LDT(L_{right})$;
- 9 Create a node v storing C_{mid} ;
- 10 Make v_{left} the left child of v ;
- 11 Make v_{right} the right child of v ;
- 12 **return** v ;

A linear dilution tree (LDT) is a complete binary search tree having $2^k - 1$ nodes, where each node represents a \mathcal{CF} value in the target set \mathcal{L} , where $|\mathcal{L}| = 2^k + 1$. Thus, the tree will have a depth of $(k - 1)$, where the root is assumed to be at depth 0.

Algorithm 1 builds LDT from the input target set, on which Algorithm 2 described below, will be run to produce the droplets in the target set \mathcal{L} .

Algorithm 2: Linear dilution

Input: $\mathcal{L} = \{\frac{a}{2^n}, \frac{a+d}{2^n}, \frac{a+2d}{2^n}, \dots, \frac{a+2^k d}{2^n}\}$
Output: Output ordering of \mathcal{CF} s in \mathcal{L}

- 1 $\mathcal{L}' = \{\frac{a+d}{2^n}, \frac{a+2d}{2^n}, \dots, \frac{a+(2^k-1)d}{2^n}\}$;
 $\triangleright \frac{a}{2^n}$ and $\frac{a+2^k d}{2^n}$ have unlimited supply;
- 2
- 3 $root = LDT(\mathcal{L}')$;
- 4 **return** $postorder(root)$;
- 5 $\triangleright postorder(root)$ is the post-order traversal of the binary tree;

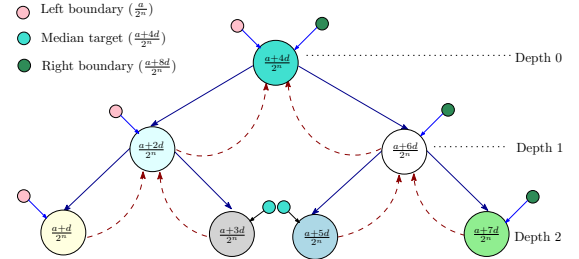


Fig. 2: Linear dilution tree

B. An illustrative example

As an illustration, let us consider $k = 3$. Let $\mathcal{T}_{linear} = \{\frac{a}{2^n}, \frac{a+d}{2^n}, \frac{a+2d}{2^n}, \dots, \frac{a+2^3 d}{2^n}\}$ be a linear gradient of targets to be generated from $\frac{0}{2^n}$ and $\frac{2^n}{2^n}$, i.e., $|\mathcal{T}_{linear}| = 2^3 + 1 = 9$. The corresponding (LDT) is shown in Fig. 2, which is generated by Algorithm 1. We traverse the tree in depth-first order and produce the droplets in a post-order mixing sequence. We assume that the two boundary \mathcal{CF} s $\frac{a}{2^n}$ and $\frac{a+2^3 d}{2^n}$ are supplied. Initially, we generate two droplets with \mathcal{CF} $\frac{a+4d}{2^n}$ by mixing one droplet of $\frac{a}{2^n}$ and $\frac{a+8d}{2^n}$ each (represented as the root in Fig. 2). One of these droplets is stored and the other one is mixed with $\frac{a}{2^n}$ to produce two droplets of $\frac{a+2d}{2^n}$. Again, one of them is stored and the other one is mixed with $\frac{a}{2^n}$ to generate two droplets of $\frac{a+d}{2^n}$ (leftmost leaf), out of which one droplet is sent to the output and the other one is stored. Next, the two droplets with \mathcal{CF} $\frac{a+2d}{2^n}$ and $\frac{a+4d}{2^n}$, which were stored in the first two steps, are mixed to produce two droplets of $\frac{a+3d}{2^n}$. One of them is sent to the output; the remaining one is mixed with the one with \mathcal{CF} $\frac{a+d}{2^n}$ stored in the third step. This step regenerates two droplets with \mathcal{CF} $\frac{a+2d}{2^n}$, which were consumed in earlier steps. One of them is stored again and now the other one is transported to the output. Similar *mix-split* sequences are performed on the right half of LDT in post-order fashion, and finally, two droplets of $\frac{a+4d}{2^n}$ (represented as the root) are regenerated by mixing $\frac{a+6d}{2^n}$ with $\frac{a+2d}{2^n}$. It may be observed that *no waste droplet* is produced for generating the entire linear dilution sequence \mathcal{T}_{linear} . Only one droplet for every non-boundary \mathcal{CF} value in the gradient is produced, excepting the median one, for which two droplets are produced.

The following observations are now immediate.

Observation 1. *The droplets with boundary \mathcal{CF} s are used only along the leftmost and the rightmost root-to-leaf path in LDT.*

Observation 2. *The droplets with the \mathcal{CF} values correspond-*

ing to each internal node of *LDT* are used in subsequent mixing operations after their production and are regenerated later for replenishment.

Lemma 1. *The number of copies of each droplet generated at depth i during the process is $2^{k-i} + 2$ when $i < k$, and is 2 when $i = k$ (leaf node), where $|\mathcal{L}| = 2^{k+1} + 1$.*

Proof: We proof the lemma using induction on k , i.e., the target set size $|\mathcal{L}| = 2^{k+1} + 1$.

Basis: For $k = 1$, $|\mathcal{L}| = 2^{1+1} + 1 = 5$; in this case, we need to generate 3 \mathcal{CF} values from 2 boundary concentrations. Fig. 3 shows the linear dilution tree. The total number of droplets corresponding to the median target \mathcal{CF} (at the root, depth = 0) is $4(= 2 + 2)$ and target concentration at depth 1 is 2 each. Hence the Lemma 1 is true for $k = 1$.

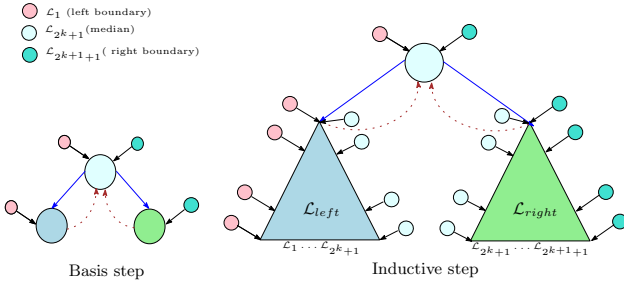


Fig. 3

Induction hypothesis: Assume the statement is true for all $m \leq k - 1$.

Inductive steps: Consider the target set \mathcal{L} of size $2^{k+1} + 1$ i.e., $m = k$. One can split \mathcal{L} into three parts: \mathcal{L}_{left} that contains the first $2^k + 1$ targets of \mathcal{L} i.e., $\mathcal{L}_{left} = \{\mathcal{L}_1, \dots, \mathcal{L}_{2^k+1}\}$; $\mathcal{L}_{median} = \{\mathcal{L}_{2^k+1}\}$; $\mathcal{L}_{right} = \{\mathcal{L}_{2^k+1}, \dots, \mathcal{L}_{2^{k+1}+1}\}$. The elements in \mathcal{L}_{left} can be generated by using \mathcal{L}_1 and \mathcal{L}_{2^k+1} as boundary targets. Similarly, those in \mathcal{L}_{right} can be generated by using \mathcal{L}_{2^k+1} and $\mathcal{L}_{2^{k+1}+1}$ as boundary targets. One can easily generate \mathcal{L} by using \mathcal{L}_1 and $\mathcal{L}_{2^{k+1}+1}$ as boundary targets (see Fig. 3). By induction hypothesis, the number of each droplet generated during the process at depth i of \mathcal{L}_{left} and \mathcal{L}_{right} is $2^{k-1-i} + 2$ when $i < k - 1$, and is 2 when $i = k - 1$. Ignoring the regeneration part, the number of each droplet generated during the process at depth i of \mathcal{L}_{left} and \mathcal{L}_{right} is 2^{k-1-i} when $i < k - 1$, and is 2 at depth $k - 1$. From Observation 1 it follows that \mathcal{L}_{median} is used only in the rightmost path of \mathcal{L}_{left} and in the leftmost path of \mathcal{L}_{right} as shown in Fig. 3. By inductive hypothesis, the total number of droplets generated (ignoring the regeneration part) is $2 \times (\sum_{i=0}^{k-2} 2^{k-1-i} + 2) = 4 \times (\sum_{i=0}^{k-2} 2^i + 1) = 4 \times (2^{k-1} - 1 + 1) = 4 \times 2^{k-1}$. Hence, the required number of \mathcal{L}_{median} droplets is $\frac{4 \times 2^{k-1}}{2} = 2^k$. Since the number of regenerated droplets is 2, the total number of droplets generated at the root (depth = 0) is $2^k + 2$. This completes the proof. ■

Lemma 2. *The number of each boundary droplet required is 2^k for $k \geq 1$, where $|\mathcal{L}| = 2^{k+1} + 1$.*

Proof: From Observation 1 it follows that boundary droplets are needed only for the nodes lying on the leftmost and rightmost paths of *LDT*. Note that the regeneration process for an internal node does not require any boundary droplet. So the number of droplets generated excluding regeneration, is 2^{k-i} at depth i and is 2 at depth k , along the left- or rightmost path in *LDT*. The total number of droplets along these paths is $\sum_{i=0}^{k-1} 2^{k-i} + 2$. Hence, the total number of required boundary droplets will be given by

$$\frac{\sum_{i=0}^{k-1} 2^{k-i} + 2}{2} = \left(\sum_{i=0}^{k-1} 2^i \right) + 1 = (2^k - 1) + 1 = 2^k$$

Theorem 1. *Algorithm 2 generates a linear dilution gradient $|\mathcal{L}| (= 2^{k+1} + 1)$ in $2^{k-1}(k + 4) - 1$ (1 : 1) mix-split steps without producing any waste droplets, when 2^k droplets of each boundary \mathcal{CF} are supplied.*

Proof: The *LDT* has $2^{k+1} - 1$ nodes including 2^k leaf nodes. Each leaf node requires only one *mix-split* operation. By Lemma 1 the number of each droplet generated at depth i is $2^{k-i} + 2$ for $0 \leq i \leq k - 1$, where the constant 2 accounts for its regeneration from its two children. Regeneration requires $2^k - 1$ *mix-split* steps. Hence the total number of *mix-split* operations will be

$$\begin{aligned} & 2^k + \frac{\sum_{i=0}^{k-1} 2^{k-i} \times 2^i}{2} + 2^k - 1 \\ &= 2^k + \frac{\sum_{i=0}^{k-1} 2^k}{2} + 2^k - 1 \\ &= 2^{k+1} + k \cdot 2^{k-1} - 1 \\ &= 2^{k-1}(k + 4) - 1 \end{aligned}$$

The fact that no waste droplet is generated in this process follows easily by counting the number of input droplets (Lemma 2) and the output droplets. ■

Observation 3. *The \mathcal{CF} values of the gradient excluding the two boundary \mathcal{CF} s appear at the output of the generator in accordance to the post-order traversal sequence of *LDT*.*

The following theorem provides an upper bound on the storage requirement during gradient generation.

Theorem 2. *Algorithm 2 requires at most $2k$ storage electrodes at any instant of time, where $|\mathcal{L}| = 2^{k+1} + 1$.*

Proof: We proof the lemma using induction on k .

Basis: For $k = 1$, $|\mathcal{L}| = 2^{1+1} + 1 = 5$. One needs to generate three \mathcal{CF} s from 2 boundary concentrations. It is easy to check that we require at most 2 intermediate storage elements in this case. Hence the theorem is true for $k = 1$.

Inductive hypothesis: Assume the statement is true for $k - 1$.

Inductive steps: Consider the target set \mathcal{L} of size $2^{k+1} + 1$. One can split \mathcal{L} into three parts: \mathcal{L}_{left} that contains the first $2^k + 1$ targets of \mathcal{L} , i.e., $\mathcal{L}_{left} = \{\mathcal{L}_1, \dots, \mathcal{L}_{2^k+1}\}$; \mathcal{L}_{median} that contains the median target of \mathcal{L} ; $\mathcal{L}_{right} = \{\mathcal{L}_{2^k+1}, \dots, \mathcal{L}_{2^{k+1}+1}\}$ (see Fig. 3). By inductive hypothesis,

the left subtree requires $2(k-1)$ storage. Additionally, we need to store one droplet of $\mathcal{CF}(\mathcal{L}_{2^{k+1}})$ corresponding to the root. So, a total of $2(k-1) + 1 = 2k - 1$ storage is required in order to generate all the \mathcal{CF} s on the left subtree.

When we generate the target set for the right subtree, we need to store the root \mathcal{CF} of the left subtree for regeneration purpose. By analogous argument, we can claim the right subtree requires $2k - 1$ storage. Hence, the total number of storage required is $(2k - 1) + 1 = 2k$ for a linear dilution tree of size $|\mathcal{L}| = 2^{k+1} + 1$. ■

C. Generation of boundary droplets

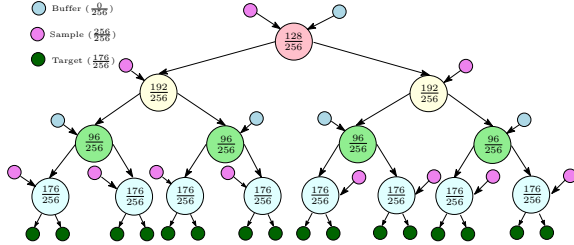


Fig. 4: Generation of a target \mathcal{CF} with multiple demand

In order to produce a dilution gradient of size $2^{k+1} + 1$, we need to supply 2^k droplets for each boundary \mathcal{CF} (Lemma 2). Here, we demonstrate how a low-cost dilution engine [26] can be integrated on-chip for this purpose. We will illustrate the technique using the following example. Let $\frac{176}{256}$ be a boundary \mathcal{CF} . The corresponding dilution tree is shown in the Fig. 4. Each root-to-leaf path represents a sequence of *mix-split* operations needed to generate the droplet by applying the *BS* method. One can store the intermediate droplets into a stack and generate two target droplets each time by repeatedly mixing the droplet on top of the stack with either sample or buffer as needed. The dilution tree in Fig. 4 has 16 target droplets generated therein. To admit a maximum error of $\frac{1}{2^{n+1}}$, an n -depth dilution tree would suffice, and hence the number of storage elements needed to produce multiple droplets with the given \mathcal{CF} will be at most $n - 1$ [26].

D. Generation of linear gradient sequence of arbitrary length

If the number of elements in the gradient is not of the form $2^{k+1} + 1$, the above procedure needs certain modification. Let $\text{Bin}(x, m)$ denote the m -bit binary representation of x and $ZC(\text{Bin}(x, m))$ denote the number of 0's between leftmost and rightmost 1 in it. To illustrate the modification, let us assume that the target set be $\mathcal{L} = \{\mathcal{L}_0, \mathcal{L}_1, \dots, \mathcal{L}_{10}\}$, i.e., $|\mathcal{L}| = 11$. We consider another target set $\mathcal{L}' = \{\mathcal{L}_0, \mathcal{L}_1, \dots, \mathcal{L}_{16}\}$ of size $2^{2+2} + 1 = 17$. Fig. 5a shows the dilution tree for \mathcal{L}' , where the extra part of the tree is not generated (shown as dotted). Clearly, $2^{2+1} + 1 < |\mathcal{L}'| < 2^{2+2} + 1$, i.e., $k = 2$. Now, $\text{Bin}(|\mathcal{L}'| - 1, 4) = 1010$ and the number of *waste droplets* is equal to $ZC(\text{Bin}(10, 4)) = 1$ (\mathcal{L}_{12}).

The following theorem can be proved easily.

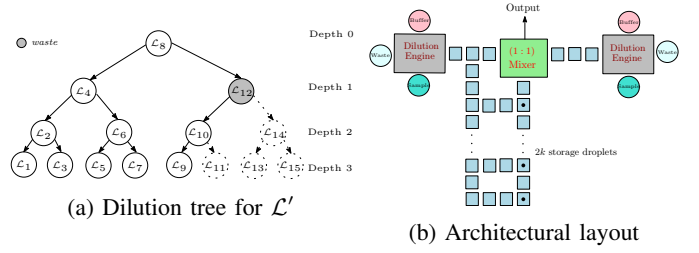


Fig. 5: (a)-Dilution tree for \mathcal{L}' (b)-Architectural layout

Theorem 3. *The number of waste droplets produced while generating \mathcal{L} is equal to $ZC(\text{Bin}(|\mathcal{L}| - 1, k + 2))$, where $2^{k+1} + 1 < |\mathcal{L}| < 2^{k+2} + 1$. □*

V. ARCHITECTURE

An architectural layout for producing a linear dilution gradient is shown in Fig. 5b. If boundary \mathcal{CF} s other than 0% and 100% are needed, a dilution engine [26] can be used for generating them. We provide two dilution engines for generating the boundary \mathcal{CF} s, which can be run in parallel to reduce sample preparation time. Each dilution engine is equipped with a stack of $(n - 1)$ storage droplets in order to increase the throughput of boundary droplets and to reduce the number of *waste* droplets. The detailed layout of the dilution engine can be found elsewhere [26]. To generate the gradient part, we use one (1 : 1) mix-split module and $2k$ additional storage cells (Theorem 2). Thus, to produce a gradient of size $|\mathcal{L}| = 2^{k+1} + 1$, with a maximum error of $\frac{1}{2^{n+1}}$ in each of the target \mathcal{CF} , one needs a total of $2(n + k - 1)$ storage electrodes. The overall execution time for generating the gradient can further be minimized by adopting a scheduling algorithm [27] for the best utilization of resources.

VI. SIMULATION RESULTS

We have performed extensive simulation on various target sets (Table I) and calculated the number of (1 : 1)-*mix-split* steps and *waste* droplets. We have compared our results with the methods of Mitra et al. [17], Hsieh et al. [16], and Huang et al. [18]. The results are shown in Table II. The number of *waste* droplets in *LDT* for the proposed method is shown within parentheses in Table II along with total *mix-split* steps (\mathcal{M}) and *waste* (\mathcal{W}) droplets.

TABLE I: Target set ($n = 10$)

	TS size	Target set
TS_1	5	$\{\frac{50}{2^{10}}, \frac{70}{2^{10}}, \dots, \frac{130}{2^{10}}\}$
TS_2	10	$\{\frac{110}{2^{10}}, \frac{120}{2^{10}}, \dots, \frac{200}{2^{10}}\}$
TS_3	17	$\{\frac{20}{2^{10}}, \frac{70}{2^{10}}, \dots, \frac{820}{2^{10}}\}$
TS_4	20	$\{\frac{40}{2^{10}}, \frac{70}{2^{10}}, \dots, \frac{610}{2^{10}}\}$

In our experiments, we have considered 6 different linear dilution gradient sets \mathcal{L} of size $2^k + 1$ for $k = 2, \dots, 7$. For each k , we have chosen 100 random sets in the range of $\frac{1}{1024}$ and $\frac{1023}{1024}$, assuming $n = 10$. Hence the error in concentration factors will be at most $\frac{1}{2048}$. Assuming 100%

TABLE II: The number of *mix-split* steps & *waste* droplets

TS	Proposed		Mitra et al.		Hsieh et al.		Huang et al.	
	\mathcal{M}	\mathcal{W}	\mathcal{M}	\mathcal{W}	\mathcal{M}	\mathcal{W}	\mathcal{M}	\mathcal{W}
$n = 10$								
TS_1	24	14 (0)	33	28	37	28	32	12
TS_2	40	13 (2)	64	54	55	36	64	22
TS_3	57	12 (0)	88	71	82	50	104	39
TS_4	65	10 (2)	108	88	95	58	126	49

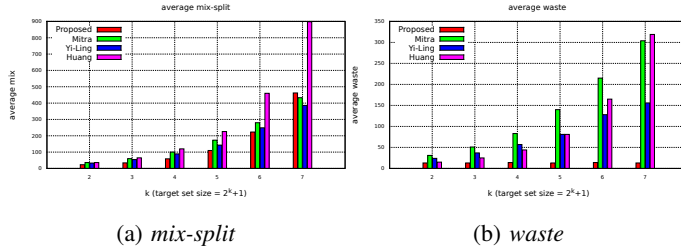


Fig. 6: Comparison of the proposed method with Mitra et al. [17], Hsieh et al. [16], and Huang et al. [18]

sample and 0% buffer as the two boundary CF s, we have counted the total number of $(1:1)$ -*mix-split* steps and *waste* droplets considering both the dilution engines and the gradient generator. Comparative results with respect to earlier methods are shown as histograms in Fig. 6, where the horizontal axis indicates the size of the target set ($|\mathcal{L}| = 2^k + 1$) for $k = 2, \dots, 7$, and the vertical axis represents the average number of *mix-split* steps and *waste* droplets required in these methods. Note that the most of the *waste* droplets that are generated in our method correspond to those produced by the dilution engines. We observe that our method produces a significantly fewer number of *waste* droplets compared to all the three earlier methods. Further, the proposed method performs better in terms of the number of *mix-split* steps up to a target set of size 65, i.e., up to $k = 6$.

VII. CONCLUSIONS

We have presented an algorithm for generating linear dilution gradients on a digital microfluidic platform. When the boundary concentration factors of a gradient of size $|\mathcal{L}| = 2^k + 1$ are supplied, our method produces the rest without generating any waste droplet, thereby saving costly stock solutions. For other gradient sizes, it produces only a few waste droplets. We have also designed a suitable layout architecture to implement the generator on-chip. Our method is adaptive to the size of dilution gradient as well to the desired accuracy of concentration factor. Thus, the proposed approach will provide a flexible and programmable environment for catering to any need of arbitrary linear gradient during sample preparation. Generation of other dilution gradients such as parabolic or sinusoidal with a digital microfluidic biochip may be studied as a future problem.

REFERENCES

- [1] M. G. Pollack, R. B. Fair, and A. D. Shenderov, "Electrowetting-based actuation of liquid droplets for microfluidic applications," *Applied Physics Letters*, vol. 77, no. 11, pp. 1725–1726, Sept. 2000.

- [2] D. Brassard, L. Malic, C. Miville-Godin, F. Normandin, and T. Veres, "Advanced EWOD-based digital microfluidic system for multiplexed analysis of biomolecular interactions," in *Micro Electro Mechanical Systems (MEMS)*, Jan. 2011, pp. 153–156.
- [3] R. B. Fair, A. Khlystov, T. D. Taylor, V. Ivanov, R. D. Evans, V. Srinivasan, V. K. Pamula, M. G. Pollack, P. B. Griffin, and J. Zhou, "Chemical and biological applications of digital-microfluidic devices," *IEEE Design & Test of Computers*, vol. 24, no. 1, pp. 10–24, 2007.
- [4] K. Chakrabarty and F. Su, *Digital Microfluidics - Synthesis, Testing, and Reconfiguration Techniques*. CRC Press, 2007.
- [5] S. K. Cho, H. Moon, and C.-J. Kim, "Creating, transporting, cutting, and merging liquid droplets by electrowetting-based actuation for digital microfluidic circuits," *Microelectromechanical Systems, Journal of*, vol. 12, no. 1, pp. 70–80, Feb. 2003.
- [6] Y. Fouillet, D. Jary, C. Chabrol, P. Claustre, and C. Peponnet, "Digital microfluidic design and optimization of classic and new fluidic functions for lab on a chip systems," *Microfluidics and Nanofluidics*, vol. 4, pp. 159–165, 2008.
- [7] J. Berthier, *Micro-Drops and Digital Microfluidics*. Elsevier, Feb. 2008.
- [8] S. Sugiura, K. Hattori, and T. Kanamori, "Microfluidic serial dilution cell-based assay for analyzing drug dose response over a wide concentration range," *Analytical Chemistry*, vol. 82, no. 19, pp. 8278–8282, 2010.
- [9] G. V. Doern, R. Vautour, M. Gaudet, and B. Levy, "Clinical impact of rapid in vitro susceptibility testing and bacterial identification," *Journal of Clinical Microbiology*, vol. 32, no. 7, pp. 1757–1762, July 1994.
- [10] M. J. Jebrail and A. R. Wheeler, "Digital microfluidic method for protein extraction by precipitation," *Analytical Chemistry*, vol. 81, no. 1, pp. 330–335, 2009.
- [11] X. Chen, D. Cui, C. Liu, H. Li, and J. Chen, "Continuous flow microfluidic device for cell separation, cell lysis and dna purification," *Analytica Chimica Acta*, vol. 584, no. 2, pp. 237–243, 2007.
- [12] K. Lee, C. Kim, G. Jung, T. Kim, J. Kang, and K. Oh, "Microfluidic network-based combinatorial dilution device for high throughput screening and optimization," *Microfluidics and Nanofluidics*, vol. 8, pp. 677–685, 2010.
- [13] S. Wang, N. Ji, W. Wang, and Z. Li, "Effects of non-ideal fabrication on the dilution performance of serially functioned microfluidic concentration gradient generator," in *Nano/Micro Engineered and Molecular Systems (NEMS)*, 2010, pp. 169–172.
- [14] S. K. W. Dertinger, D. T. Chiu, N. L. Jeon, and G. M. Whitesides, "Generation of gradients having complex shapes using microfluidic networks," *Analytical Chemistry*, vol. 73, no. 6, pp. 1240–1246, 2001.
- [15] Y.-H. Jang, M. J. Hancock, S. B. Kim, S. Selimovic, W. Y. Sim, H. Bae, and A. Khademhosseini, "An integrated microfluidic device for two-dimensional combinatorial dilution," *Lab Chip*, vol. 11, pp. 3277–3286, 2011.
- [16] Y.-L. Hsieh, T.-Y. Ho, and K. Chakrabarty, "A reagent-saving mixing algorithm for preparing multiple-target biochemical samples using digital microfluidics," *IEEE Trans. on CAD of Integrated Circuits and Systems*, vol. 31, no. 11, pp. 1656–1669, 2012.
- [17] D. Mitra, S. Roy, K. Chakrabarty, and B. B. Bhattacharya, "On-chip sample preparation with multiple dilutions using digital microfluidics," in *ISVLSI*, 2012, pp. 314–319.
- [18] J.-D. Huang, C.-H. Liu, and T.-W. Chiang, "Reactant minimization during sample preparation on digital microfluidic biochips using skewed mixing trees," in *Computer-Aided Design (ICCAD), 2012 IEEE/ACM International Conference*, Nov. 2012, pp. 377–383.
- [19] H. Ren, V. Srinivasan, and R. Fair, "Design and testing of an interpolating mixing architecture for electrowetting-based droplet-on-chip chemical dilution," in *TRANSDUCERS, Solid-State Sensors, Actuators and Microsystems*, vol. 1, 2003, pp. 619–622.
- [20] G. M. Walker, N. Monteiro-Riviere, J. Rouse, and O. T. Neill, "A linear dilution microfluidic device for cytotoxicity assays," in *Lab Chip*, vol. 7, 2010, pp. 226–232.
- [21] A. O'Neill, N. Monteiro-Riviere, and G. Walker, "A serial dilution microfluidic device for cytotoxicity assays," in *Engineering in Medicine and Biology Society*, Sept. 2006, pp. 2836–2839.
- [22] K. Lee, C. Kim, B. Ahn, R. Panchapakesan, A. R. Full, L. Nordee, J. Y. Kang, and K. W. Oh, "Generalized serial dilution module for monotonic and arbitrary microfluidic gradient generators," *Lab Chip*, vol. 9, pp. 709–717, 2009.
- [23] W. Thies, J. P. Urbanski, T. Thorsen, and S. P. Amarasinghe, "Abstraction layers for scalable microfluidic biocomputing," *Natural Computing*, vol. 7, no. 2, pp. 255–275, 2008.
- [24] S. Roy, B. B. Bhattacharya, and K. Chakrabarty, "Optimization of dilution and mixing of biochemical samples using digital microfluidic biochips," *IEEE Trans. on CAD of Integrated Circuits and Systems*, vol. 29, no. 11, pp. 1696–1708, 2010.
- [25] S. Bhattacharjee, A. Banerjee, and B. B. Bhattacharya, "Multiple dilution sample preparation using digital microfluidic biochips," in *ISED*, 2012.
- [26] S. Roy, B. B. Bhattacharya, S. Ghoshal, and K. Chakrabarty, "Low-cost dilution engine for sample preparation in digital microfluidic biochips," in *ISED*, 2012.
- [27] K. O'Neal, D. Grissom, and P. Brisk, "Force-directed list scheduling for digital microfluidic biochips," in *VLSI and System-on-Chip (VLSI-SoC)*, 2012.